



Numerical Analysis of Dissimilar Metal Welding

Prof. Vijaykumar Chalwa* and Prof. Sachin Kudte**

*Department of Mechanical Engineering, GSMCOE, Pune-411045 Maharashtra, India

**Department of Mechanical Engineering, GSMCOE, Pune-411045 Maharashtra, India

(Corresponding author: Prof. Vijaykumar Chalwa)

(Received 28 September, 2016 Accepted 29 October, 2016)

(Published by Research Trend, Website: www.researchtrend.net)

ABSTRACT: Joining of dissimilar metals has found its use extensively in power generation, electronic, nuclear reactors, petrochemical and chemical industries mainly to get tailor-made properties in a component and reduction in weight. However efficient welding of dissimilar metals has posed a major challenge due to difference in thermo-mechanical and chemical properties of the materials to be joined under a common welding condition. This causes a steep gradient of the thermo-mechanical properties along the weld. A variety of problems come up in dissimilar welding like cracking, large weld residual stresses, migration of atoms during welding causing stress concentration on one side of the weld, compressive and tensile thermal stresses, stress corrosion cracking, etc. Weld residual stress and thermal stress have been analysed for dissimilar metal welding of 304 stainless steel to 1020 mild steel taking 302 stainless steel as the filler metal. Similarly taking strain developed as an index the susceptibility of the welded joint to stress corrosion cracking have been studied. It is found that when the filler metal is replaced by Inconel 625 significant improvement is obtained in the welded joint in terms of reduction in stress developed and stress corrosion cracking. Also the problem of carbon migration is eliminated by the use of Inconel 625 as a weld filler metal due to the resistance of nickel-based alloys to any carbon diffusion through them.

Keywords: dissimilar welding; stress corrosion cracking; thermal stress; residual stress.

I. INTRODUCTION

Welding is a manufacturing process of creating a permanent joint obtained by the fusion of the surface of the parts to be joined together, with or without the application of pressure and a filler material. The materials to be joined may be similar or dissimilar to each other. The heat required for the fusion of the material may be obtained by burning of gas or by an electric arc. The latter method is more extensively used because of greater welding speed.

Weld Processes. The welding processes may be broadly classified into the following two groups:

1. Welding processes that use heat alone i.e. Fusion Welding.
2. Welding processes that use a combination of heat and pressure i.e. Forge Welding.

Fusion Welding. In case of fusion welding the parts to be joined are held in position while the molten metal is supplied to the joint. The fusion welding, according to the method of heat generated, may be classified as:

1. Thermite Welding
2. Gas Welding
3. Electric Arc Welding

Forge Welding. In forge welding, the parts to be joined are first heated to a proper temperature in a furnace and then hammered. Electric Resistance Welding is an example of forge welding.

Welded Joints. The welding joint geometry can be classified primarily into five types. The various joints are shown in the figure 1 below:

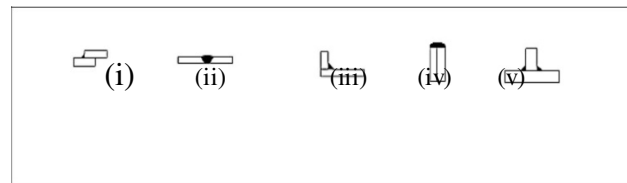


Fig. 1. Types of Welded Joints.

- | | |
|-------|--------------|
| (i) | Lap Joint |
| (ii) | Butt Joint |
| (iii) | Corner Joint |
| (iv) | Edge Joint |
| (v) | T-Joint |

The aim of this research project has been to study dissimilar metal joint using a filler metal. Dissimilar welding is used to fabricate the pressure vessels and piping in power plant but failures occur frequently due to:

1. Thermal Stress which is generated due to difference in co-efficient of thermal expansion.

2. Difference in mechanical properties, the local heating and subsequent cooling results in large residual stress.

The metals to be welded are 304 stainless steel and 1020 plain carbon steel and the filler metal used is 302 Stainless steel whose properties has been taken similar to 304 stainless steel for the purpose of analysis. The welding process has been simulated using finite element analysis. The software used for this analysis is ANSYS 13.0 using its Workbench module. It is because Workbench is a very powerful tool to simulate a welding joint and infer the results. Also it has a reputation of coming up with results very close to the practical values. The input parameters are easily fed and boundary conditions, geometrical modelings are very convenient due to its user-friendly graphic interface.

Problem Statement. The problems which have been analysed in this research are three. First aspect is reduction in stresses developed, second is minimization of carbon migration and the third is decreasing the susceptibility to Stress Corrosion Cracking. Considering the above objectives two metal plates, equal in size with a dimension of 300 x 150 x 8 mm are butt welded with filler between them. The parent metal plates are of 304 stainless steel and 1020 mild steel material. The welding arrangement has been shown in Fig 5.

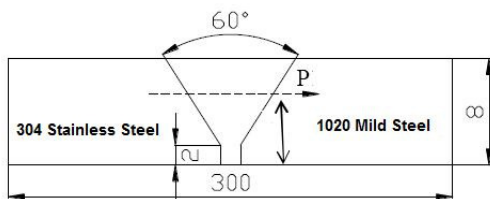


Fig. 5. Schematic representation of the welded joint.

The welding simulation has been done firstly by studying the welding temperature field followed by incrementally applying the temperature results to simulate the weld. After the welding process is over residual stresses get developed inside the welded parts. This welded part when kept under operating conditions which are taken as high as 600 °C, results in development of thermal stresses inside the welded part. The analysis has been done considering three models. Model A is analysed only for thermal stresses and the results are inferred. Model B is analysed only for residual stresses and the results are inferred. Model C is

analysed for thermal stresses superimposed with residual stresses. That means mathematically-

$$\text{Model A} + \text{Model B} = \text{Model C}$$

And all the results are taken along the line of length 30mm which lies 5mm above the weld root. Now in the second case, the weld metal A302 Stainless Steel is changed to Inconel 625 and then again the thermal, residual and thermal stress superimposed on residual stresses are calculated.

RESULTS AND DISCUSSION

The results that are obtained after the weld simulation can be taken considering two cases. In the first case 302 stainless steel has been taken as the weld filler metal whose properties are taken the same as 304 stainless steel which is one of the parent metals. So the results inferred from all the three models viz. A, B and C which will be taken one by one.

Case I

30 Stainless Steel as Weld Filler Metal

Thermal stress has developed inside the welded part as both of its ends across the weld have been fixed against any kind of motion by setting up in nodal displacement in all directions as zero. This is the boundary conditions used in model A and model C. Considering Model A, where only the part has been subjected to thermal stresses the results are explained in the figures below. The figures below show the stress contour near the weld metal and the graphs which are path results along the line of length 30 mm at the centre of the filler metal and at a distance of 5 mm from the weld root. The line is called line P in the subsequent paragraphs.

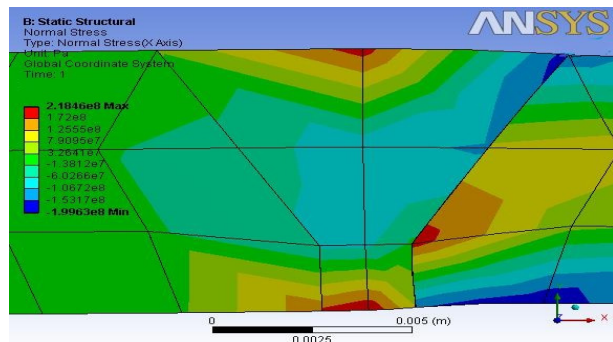


Fig. 6. Normal stress contour of Model A.

The normal stress varies from 218 MPa tensile to 199 MPa compressive. The peak of the tensile lies along the centerline of the weld metal. However peak of the compressive stress lies in the weld interface of weld filler metal and 1020 mild steel.

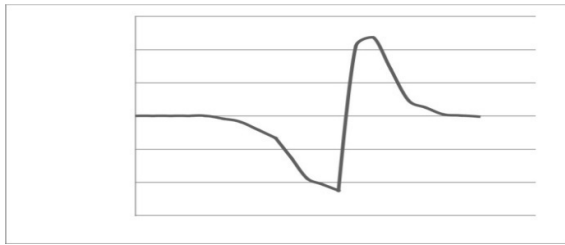


Fig. 7. Normal stress distribution along line P.

The normal stress along the line P in both directions is found in the weld interface near the 1020 mild steel. The maximum stress is found to be 118 MPa in the tensile direction.

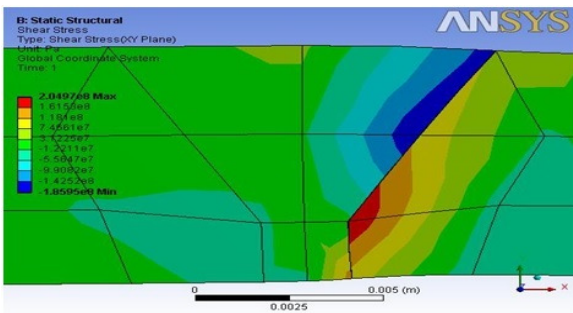


Fig. 8. Shear stress contour of Model A.

The shear stress varies from 204 MPa positive to 186 MPa negative. However peak of the shear stress lies in the weld interface of weld filler metal and 1020 mild steel. From the above two cases it is very clear that the weld interface on the 1020 mild steel is the highest risk zone, where the failure is most likely to occur. The shear stress distribution along the line P is shown in Fig. 9.

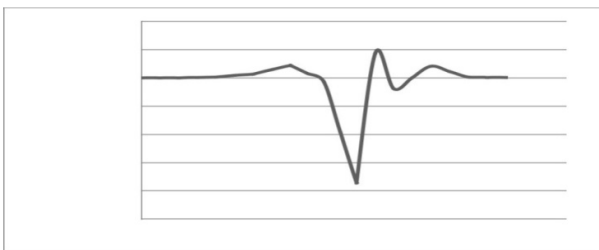


Fig. 9. Shear stress distribution along line P.

The maximum shear stress along the line P is 186 MPa along the negative direction and also is located in the weld interface on 1020 mild steel side. Now taking up the case where residual stresses have developed as a result of heating and subsequent cooling during the welding process.

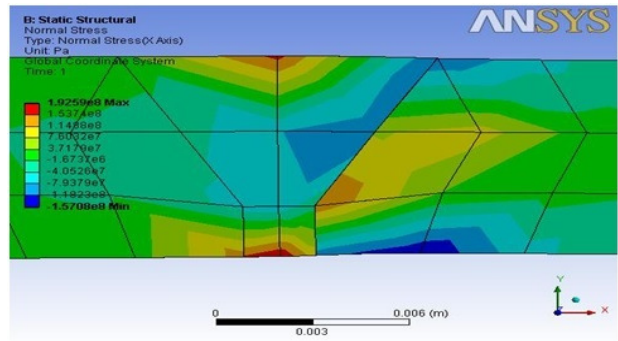


Fig. 10. Normal stress contour of Model B.

The normal stress varies from 192 MPa tensile to 157 MPa compressive. The peak of the tensile lies on the 1020 mild steel and compressive stress lies in the 304 stainless steel side. This is due to larger coefficient of thermal expansion of 304 stainless steel. The stress gradient in the filler metal is very steep due to rapid change in the direction of stresses

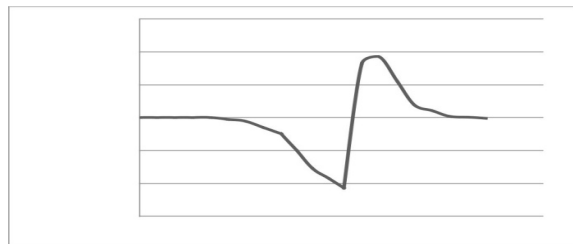


Fig. 11. Normal stress distribution along line P.

The maximum stress is induced in the weld interface on the 1020 mild steel side and its magnitude is 107 MPa and is of compressive nature. The steep gradient in the stress in this zone represents the vulnerability of this zone to cracking.

Similarly the shear stress contour in the XY-plane developed in the model B is shown in the Fig. 12.

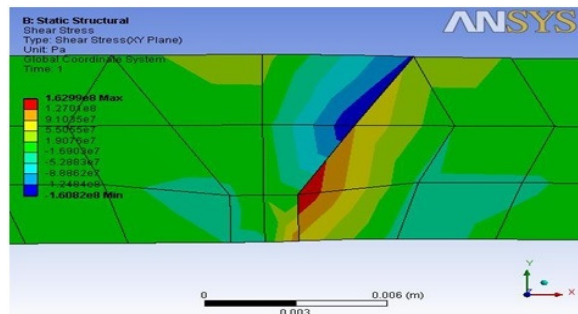


Fig. 12. Shear stress contour of Model B.

The shear stress varies from 204 MPa positive to 186 MPa negative. However peak of the shear stress lies in the weld interface of weld filler metal and 1020 mild steel. The extremes of stress in both directions also lie in the same location making it the weakest part.

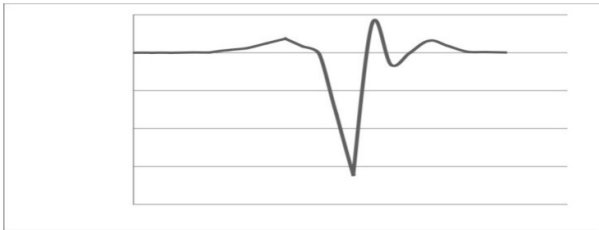


Fig. 13. Shear stress distribution along line P.

The maximum value of shear stress along the line P is found to be 161 MPa, and the stress is in clockwise direction which is assumed to be negative direction. At the weld interface on 1020 mild steel side, shear stress rises falls very rapidly.

In the model C, where the thermal stress is superimposed on residual stress the normal stress contour developed is shown in Fig. 14.

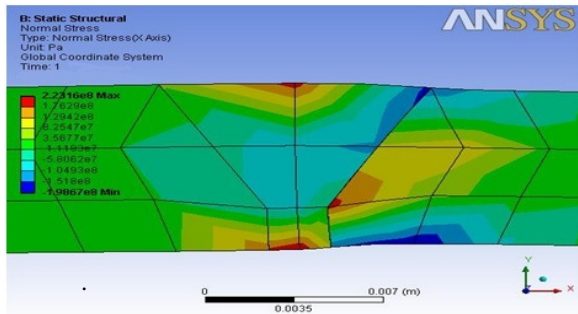


Fig. 14. Normal stress contour of Model C.

The value of normal stresses developed in the welded joint in the model C is 223 MPa of the tensile nature and 198 MPa of the compressive nature. The maximum tensile stress is located at the centre of the welded joint and is much localized.

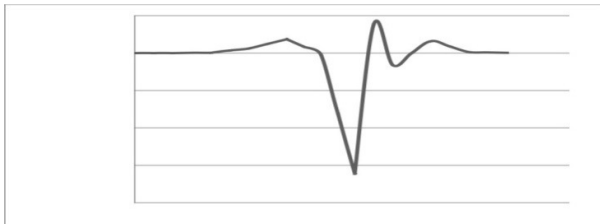


Fig. 15. Normal stress distribution along line P.

The stress distribution graph that normal stress value is highest i.e. 140 MPa near the weld interface on the 1020 mild steel side. The magnitude of stress is highest in both the directions at this very location.

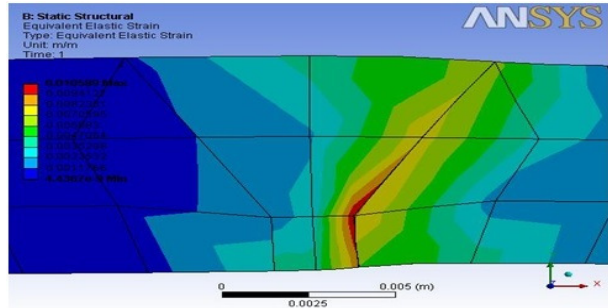


Fig. 16. Shear stress contour of Model C.

Similarly the shear stress contour in XY-plane as shown in Fig. 16 indicates a high cyclic reversal of stresses at the weld interface on 1020 mild steel side. The value of stress here varies from 205 MPa counter-clockwise to 186 MPa in the clockwise sense. By the virtue of shear stress developed it is quite clear that the welded joint is most likely to break at the weld interface on 1020 mild steel side.

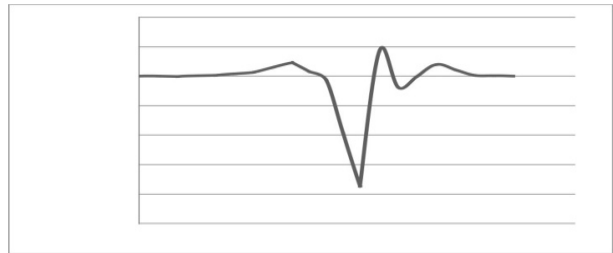


Fig. 17. Shear stress distribution along line P.

The path results obtained on the line P also confirm that there is a huge cyclic reversal of stresses in the zone mentioned above.

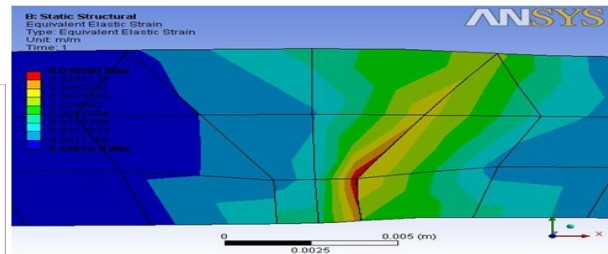


Fig 18. Equivalent strain contour in Model C.

The maximum value of shear stress i.e. 187 MPa is also present on this particular line. The analysis of strain which is a parameter in deciding the susceptibility of stress corrosion cracking is discussed in the next paragraph. In line with the stresses the contour of equivalent strain also depicts that a maximum strain of 0.01 m/m is also located in the weld interface on the 1020 mild steel side. This means that this interface has the highest deformation.

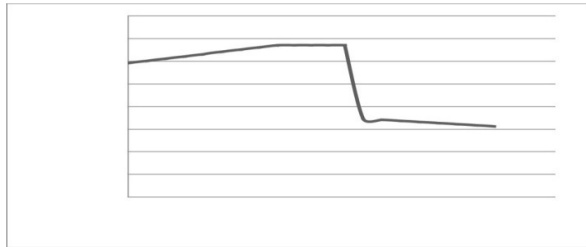


Fig 19. Equivalent strain distribution along the line P .

The value of maximum equivalent strain is 0.0335 m/m and its value remain almost constant in the HAZ of 304 stainless steel and reach its peak in the weld metal zone and then recede rapidly in the 1020 mild steel side. Having seen these problems of high stress and strain with 302 stainless steel as the weld metal, Inconel 625 replaces it for the next analysis.

**Case II
Inconel 625 as Weld Filler Metal**

Now the weld metal is changed from 302 stainless steel to Inconel 625. Inconel 625 has been chosen because of its material properties, which are intermediate between 304 stainless steel and 1020 mild steel. Again the welded joint is simulated as in case I, keeping the other entire boundary condition same.

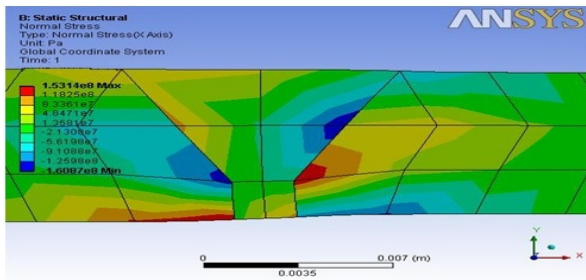


Fig. 20. Normal stress contour of Model A.

The value of stress varies from 153 MPa tensile to 160 MPa compressive. A notable change that can be observed from the previous case is that the rise in stress is not limited only in 1020 stainless steel side but a somewhat lower but appreciable rise is also seen in the 304 stainless steel side.

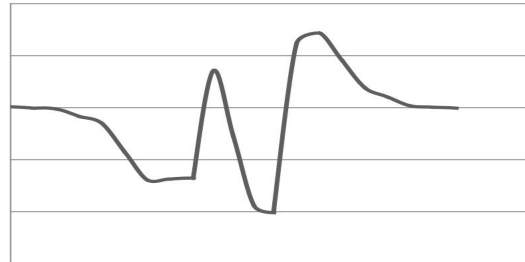


Fig. 21. Normal Stress distribution along line P.

The values of maximum stress on 304 stainless steel side is 71 MPa and while a maximum of 101 MPa is found on 1020 mild steel side.

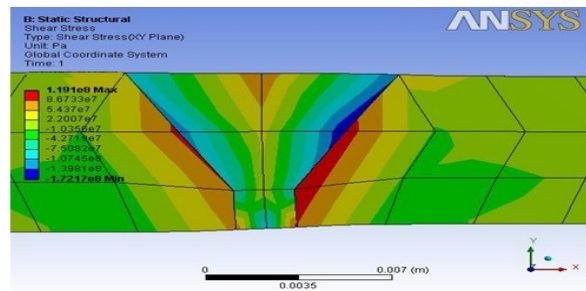


Fig. 22. Shear stress contour of Model A.

Shear stress values in the XY-plane vary from 119 MPa counter-clockwise to 172 MPa in the clockwise sense. It is to be noted that high cyclic shear stresses have developed in the weld interface on 1020 mild steel side and in terms of shear stress this side of weld metal is still the highest risk zone.

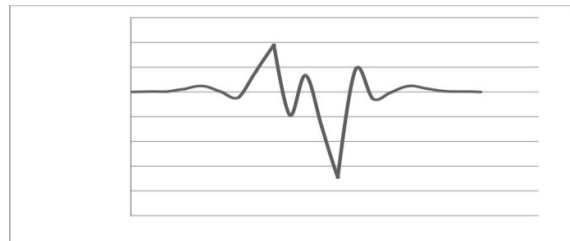


Fig. 23. Shear stress distribution along line P.

The maximum value of shear stress which is 172 MPa falls on the line P, which depicts that the weakest point falls at a distance of 5 mm from the weld root near the 1020 mild steel side.

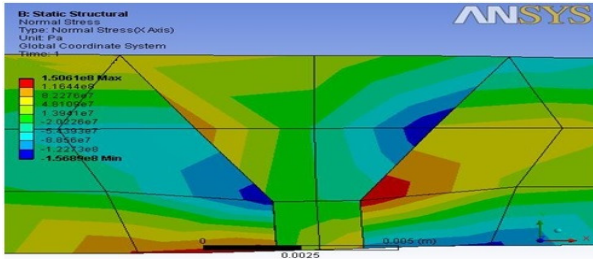


Fig. 24. Normal stress contour of Model B.

For the case wherein residual stress has developed due to cooling after welding the value of stress varies from 150 MPa in tensile sense to 156 MPa in the compressive sense.

As shown in the contour diagram tensile stresses have developed on 1020 side while 304 stainless steel and Inconel have compressive stress developed in their region.

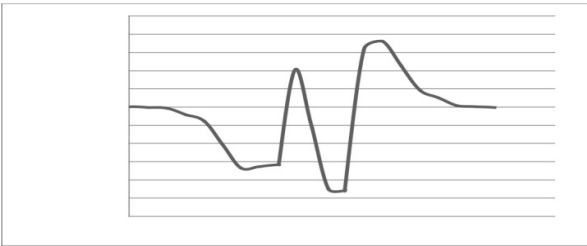


Fig. 25. Normal stress distribution along line P.

The maximum value of normal stress is found in the weld interface near the 1020 mild steel and its value is 91 MPa which is compressive in nature. However the value of stress in terms of magnitude is found to be uniformly increasing and decreasing along the weld metal.

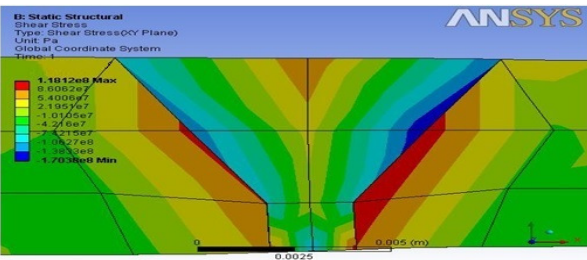


Fig. 26. Shear stress contour of Model B.

The shear stress developed in the welded part in XY-plane is 118 MPa in the counter-clockwise sense and 170 MPa in the clockwise sense. Both the peaks of clockwise and counter-clockwise are present on the weld interface on the 1020 mild steel side.

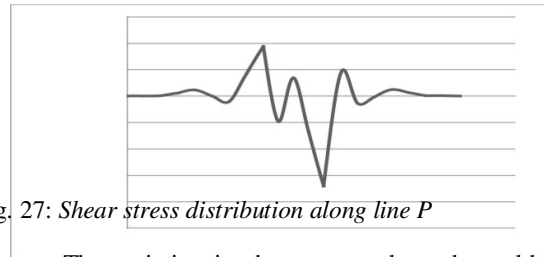


Fig. 27: Shear stress distribution along line P

The variation in shear stress along the weld metal is very rapidly changing in a cyclic fashion. The value of maximum shear stress in clockwise sense is located at the weld interface on 1020 mild steel side on the line P and its value is 170 MPa.

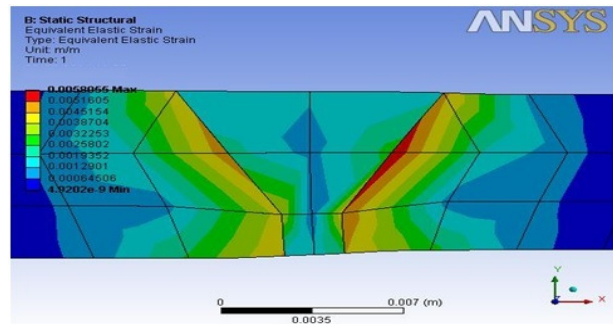


Fig. 28. Normal stress contour of Model C.

The model C which is superimposed thermal stress on residual stress the maximum normal stress has shifted away from the weld metal zone towards the side of 304 stainless steel. Even if the highest value of stress is about 155 MPa tensile and 157 MPa compressive, but still the value of normal stress in the weld metal zone is very low as depicted by Fig. 29.

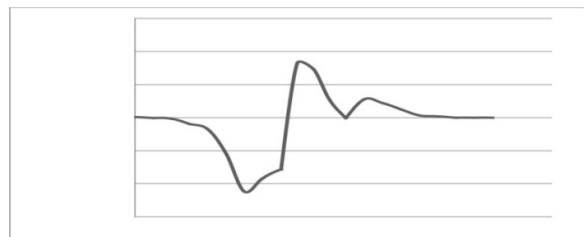


Fig. 29. Normal stress distribution along line P.

Fig. 29 shows the value of maximum normal stress of around 102 MPa along the line P, which is almost half of the maximum stress developed in the entire welded part. Almost entire of the weld zone has nearly equal value of stress as shown in Fig. 28. This is the advantage by using Inconel 625 as a weld metal which reduces the stress developed in the weld metal zone and makes the joint safer.

The cyclic variation of stress is near the 304 stainless steel side but still the value of stress is appreciably lower than that in case of 302 stainless steel as the weld metal. Now, finally considering the strain developed in the model C, it is found that the value of equivalent strain varies from 0.0058 to a minimum of 4.92e-9. The peak value of strain lies in the weld interface on the 1020 mild steel side. The values of strain are found higher only in the HAZ of parent metals and most of the weld metal has developed negligible strain.

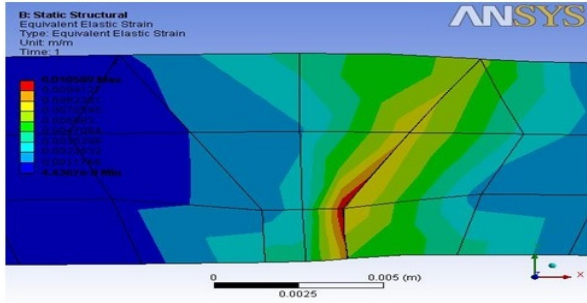


Fig. 30. Shear stress contour of Model C.

The value of the shear stress in the XY-plane developed is highest in the weld interface on the 304 stainless steel side. The value of the stress varies from 146 MPa in counter-clockwise sense and 143 MPa in clockwise sense. Even if the highest stress has changed places between the interfaces, but still its value has decreased.

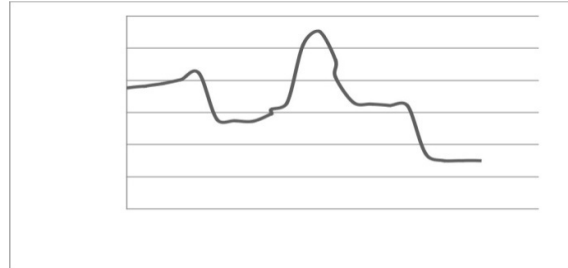


Fig. 33. Equivalent strain distribution along line P.

The equivalent strain along the line P shows higher values of strain in the heat affected zone of the parent metal and whose values decrease within the weld metal. The peak value of strain along the path is 0.0276 m/m. After getting the results, the data regarding the maximum values of normal stress along the line P is tabulated comparing both the cases of welding;

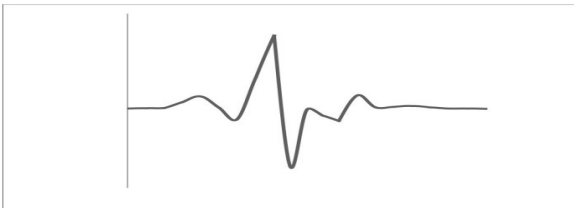


Fig. 31. Shear stress distribution along line P.

The same is depicted by Fig. 31, as the highest value of stress along the line P is found to be 92.6 MPa.

Table 10: Comparison of normal stress values in the two cases of welding.

Models	Nature of Stress	Case I: 302 Stainless Steel	Case II: Inconel 625
A	Tensile	118 MPa	71 MPa
	Compressive	112 MPa	101 MPa
B	Tensile	92 MPa	63 MPa
	Compressive	107 MPa	91 MPa
C	Tensile	127 MPa	82 MPa
	Compressive	140 MPa	112 MPa

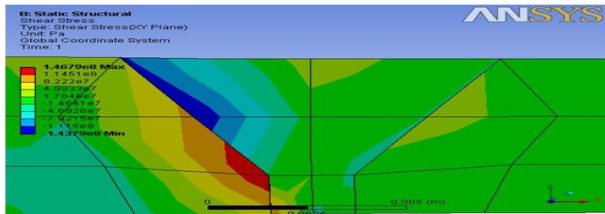


Fig. 32. Equivalent strain contour for Model C.

From the above table some of the results that can be inferred are mentioned below:

1. The maximum value of superimposed stress i.e. Model C is greater than the maximum values of both the thermal stress and weld residual stress in all the cases.
2. This explains the reason why it is necessary to consider the weld residual stress while exposing a welded part to cyclic thermal stresses. It will be an underestimation of the maximum working stress and result finally into an unsafe joint.
3. The values of stress both either of compressive or of tensile nature are found to be reduced significantly when the weld metal is changed from 302 stainless steel to Inconel 625.

It is obvious from the stress contour diagrams in the case I the highest values of stresses were in the weld interface on the 1020 mild steel side. Hence it is the weakest location the welded part.

Now from table 1 and table 2 it is clear that the carbon concentration in 1020 mild steel is much higher than that in 304 stainless steel. As a result of which, during welding or any other subsequent high temperature operation carbon atoms will diffuse from 1020 mild steel into the weld metal. So a carbon depleted zone is formed in the HAZ of 1020 mild steel and a carbon enriched zone is formed in the weld metal.

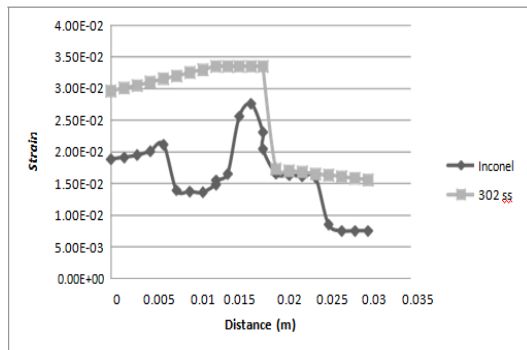


Fig. 34. Comparison of strain values between case I and case II.

Fig. 34 shows that the value of strain induced in Inconel weld metal is significantly lower than that induced in 302 stainless steel weld metal throughout the path line P. The reduction in maximum strain is 17%.

CONCLUSIONS

This research presents a study of thermal stress in a dissimilar welding joint between 1020 mild steel and 304 stainless steel, and the effect of weld residual stress

on the thermal stress has been discussed. From the results above we arrive at the following conclusions:

1. Welding which is a significant cause of residual stress generates a large amount of residual stress in the weld metal and HAZ of the parent metals, which increases the final thermal stress and should be considered while determining the strength of the joint.
2. If the residual stresses are not considered, due to lower co-efficient of thermal expansion, 1020 mild steel develops tensile thermal stress while compressive thermal stress is generated in 304 stainless steel during operating conditions.
3. The peak of the stress is reached in the weld interface of 1020 mild steel and weld metal near the mild steel side, which becomes the highest risk zone.
4. If A302 steel is replaced by Inconel 625 then the developed peak stress falls by 15-30%, and hence the welded joint becomes safer.
5. Inconel 625 is recommended to be used as the weld metal, because it also reduces strain which is an index of stress corrosion cracking as result of which the chances of stress corrosion cracking are reduced by 17%.
6. Also by introducing a weld metal which is a nickel-based alloy decreases the carbon activity gradient due to its low carbon diffusivity. Thus there is no abrupt change in material composition and hence a steep stress gradient is avoided.

A future work that can be undertaken from this research can be:

1. Superimposing fatigue loads on welded parts.
2. Introduction of a new weld metal that can still improve the results than Inconel 625 for dissimilar steels.

REFERENCES

- [1] Chengwu Yao, BinshiXu, Xiancheng Zhang, Jian, Huang, Jun Fu and YixiongWu "Interface microstructure and mechanical properties of laser welding copper-steel dissimilar joint" *Optics and Lasers in Engineering*, Vol. **47**, 2009, PP 807-814.
- [2] Wen-chun Jiang and Xue-wei Guan "A study of the residual stress and deformation in the welding between half-pipe jacket and shell" *Materials and Design*, Vol. **43**, 2013, PP 213-219.
- [3] Man Gyun Na, Jin Weon Kim and Dong Hyuk Lim "Prediction of Residual Stress for dissimilar metals welding at nuclear plants using Fuzzy Neural Network Models" *Nuclear Engineering and Technology*, Vol. **39**, 2007, PP 337-348.

- [4] M.M.A. Khan, L. Romoli, M. Fiaschi, G. Dini and F. Sarri "Laser beam welding of dissimilar stainless steels in a fillet joint configuration" *Journal of Materials Processing Technology*, Vol. **212**, 2012, PP 856-867.
- [5] Yoshiyasultoh and Kabushiki Kaisha Toshiba "Joined structure of dissimilar metallic materials" *Patent Publication Number*, EP0923145A2, 1999.
- [6] P. Delphin, I. Sattari-Far and B. Brickstad "Effect of thermal and weld induced residual stresses on the j-integral and ctod in elastic-plastic fracture analyses" *Final Report* Vol. SINTAP/SAQ/03, 1998, PP 1-47.
- [7] T.A. Mai and A.C. Spowage "Characterization of dissimilar joints in laser welding of steel-kovar, copper-steel and copper-aluminium" *Materials Science and Engineering*, Vol. **374**, 2004, PP 224-233.
- [8] Paul Colegrove, Chukwugozielkeagu, Adam Thistlethwaite, Stewart Williams, Tamas Nagy, Wojciech Suder, Axel Steuwer and Thilo Pirling "The welding process impact on residual stress and distortion" *Science and Technology of Welding and Joining*, Vol. **14**, 2009, PP 717-725.
- [9] N. Arunkumar, P. Duraisamy and S. Veeramanikandan "Evaluation Of Mechanical Properties Of Dissimilar Metal Tube Welded Joints Using Inert Gas Welding" *International Journal of Engineering Research and Applications* Vol. **2**, Issue 5, 2012, PP 1709-1717.